Int J Adv Manuf Technol (2009) 42:73–82
DOI 10.1007/s00170-008-1575-5

ORIGINAL ARTICLE

The effect of solid fraction and indirect forging pressure on mechanical properties of wrought aluminum alloy fabricated by electromagnetic stirring

C. G. Kang · S. M. Lee

Received: 20 February 2008 / Accepted: 19 May 2008 / Published online: 14 June 2008

Abstract This study demonstrated the effect of solid fraction and forging pressure on mechanical properties of the product of wrought aluminum alloys fabricated by the indirect rheoforging through electromagnetic stirring (EMS). In addition to EMS, the rheological material was examined for its response to various pouring temperatures as the rheo-material was forged into a sample which consisted parts that were directly and indirectly subjected to forge pressure. As results of investigating the relationship between microstructural features and mechanical properties of the product through microscopic inspection, the EMS rheo-forged materials revealed a fine and globular microstructure. Microstructures of Al6061 wrought aluminum alloy with uniform solid and liquid phase distributions (no segregation) demonstrated good mechanical properties with tensile strengths of up to 341 MPa.

Keywords Rheological material · Indirect forging · Electromagnetic stirring · Wrought aluminum alloy

1 Introduction

Conventional forming processes such as forging and hot forging have allowed lightweight aluminum alloys to be formed into near net shapes, but they have not been adapted to mass production due to a lack of product reliability, increased costs, and excessive initial investment. The die casting process, i.e., the forming process that fills die cavities with molten metal, has advantages for the mass production of thin parts with complex shapes, which have little need for mechanical strength. However, the process is inappropriate for producing parts with high strength requirements because defects such as turbulent flow-induced air entrapment and shrinkage could result as the melt flows into the mold cavities and also because the process reduces the die lifetime as a result of heat impact imposed on the die by overheating of the melt [1–3]. Thus, the semi-solid forming process has been developed to overcome the technical, economic, and environmental limitations caused by use of light alloy materials. The primary α-Al phase particles are controlled by rheological conditions during semi-solid processing, allowing production of critical parts for application in the transportation industry. Thus, semi-solid forming processes have been of interest as an alternate tool, mitigating the aforementioned drawbacks of traditional casting and forging processes.

Because of the numerous advantages of semi-solid processing, this sector of interest has been the subject of intensive investigation ever since the method was first suggested by Flemings in 1972 [4]. Toyoshima et al. [5] reported the finding from die casting of aluminum alloy with solid fraction of 10–40% that the higher the solid fraction, the better the quality obtained. Hirt et al. [6] concluded from rheoforging tests of aluminum alloy with a solid fraction between 40% and 80% that the die temperature should be in a range of 150–300°C to ensure that the work piece is sufficiently forged. Peng et al. [7] studied rheological behavior occurring during the rheoforming of a helically shaped workpiece. Zoqui et al. [8–10] performed a

C. G. Kang (✉)
School of Mechanical Engineering, Pusan National University,
Pusan 609-735, South Korea
e-mail: cgkang@pusan.ac.kr

S. M. Lee
Engineering Research Center for Net Shape and Die Manufacturing, Pusan National University,
Pusan 609-735, South Korea
e-mail: smlee@pnu.edu

Table 1 Chemical compositions (wt%) and thermal characteristics of aluminum alloys

	Zn	Mg	Cu	Fe	Si	Mn	Ti	Al	T_L	T_S
6061	0.03	0.98	0.30	0.15	0.62	0.03	0.01	Bal.	652°C	582°C

comparative study of the macro- and microstructural properties of A356 aluminum alloy fabricated by electromagnetic stirring (EMS) and Al6061 fabricated by EMS and thixoforging. Lee et al. [11] conducted rheoforging tests incorporating warm forging of A7075 alloy through stepwise temperature increases. Kapranos et al. [12] also studied thixoforming of wrought aluminum alloy. Ferrante et al. [13] investigated the rheological behavior of A2024 alloy and the mechanical properties of back-extruded material. Zheng et al. [14] studied the relationship between EMS operating conditions and various pouring temperatures upon the behavior of the primary α-Al phase of A356 alloy. Mao et al. [15] studied the method to fabricate slurry by EMS. Lashkari et al. [16] investigated the viscous behavior of rheo- and thixobillets of A356 aluminum alloy and suggested the functional relationship between strain and viscosity. Yoon et al. [17] investigated microstructural change in the coexistent liquid–solid phases of Al7075 alloy as a function of the isothermal holding time in the reheating process. Chayong et al. [18] and Liu et al. [19, 20] reported that the thixoforged 20xx, 60xx, and 70xx series of aluminum alloys after T6 heat treatment revealed higher strength than that of as-cast aluminum alloy. As-cast aluminum alloy has limited mechanical strength, necessitating an intensive study of rheological forging processes as applied to wrought aluminum alloy. However, a study of the forging process as it relates to the fabrication of rheological wrought aluminum alloy has not yet been reported.

Most reports in this field to date have been studies of rheological formability of as-cast aluminum alloys, which show good fluidity in liquid–solid coexistent phase. However, rheoforming of wrought aluminum alloys still remains at the research stage investigation. Therefore, this report presents a demonstration of the rheoforging of wrought aluminum alloys and characterization of the mechanical properties of arbitrary shapes, including an investigation of the distribution of the primary α-Al phase. Before indirect rheoforging, the rheological alloy is prepared by EMS. Indirect forging of rheological wrought aluminum alloys is thus carried out to investigate indirect rheo-forgibility and mechanical properties. Together with observation of workpiece microstructure, rheoforming technology can be better defined, helping to engineer parts made from high strength aluminum alloys.

2 Indirect semi-solid forging experiment

Al6061 aluminum alloy is used in this study, and its chemical composition and thermal characteristics are shown in Table 1. Al6061 alloys are widely subjected to heat treatment in which the alloys are strength-hardened through precipitation in a solid solution of Cu, Mn, Zn, and Si and in which the materials are used in near net shape process such as hot forging and extrusion [21, 22]. The main alloying elements of Al6061 aluminum alloy are Mg and Si, and the alloy is widely used in tubes and structural shapes, as it possesses good weldability and corrosion resistance. This study investigates the EMS process necessary to fabricate rheological material and the subsequent indirect forging of that material.

2.1 Fabrication of rheological material by EMS

This study investigates microstructural change with respect to the pouring temperature of aluminum alloy melt, electric current of stirring, and stirring time and also suggests optimum electromagnetic stirring conditions needed to control the grain size of molten alloys so as to forge the materials while they remain in a semi-solid state.

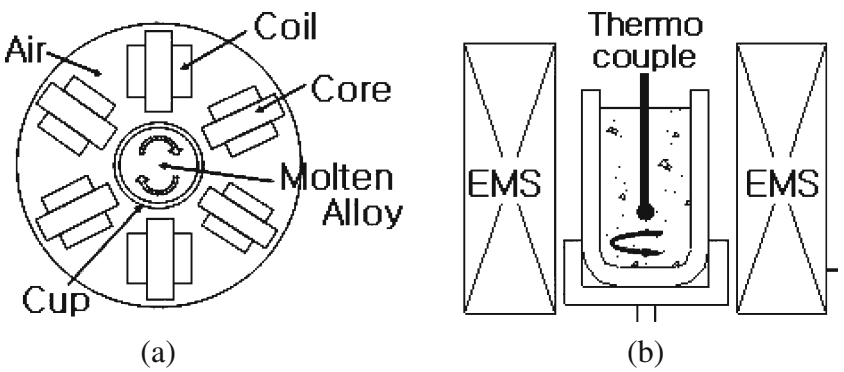

Fig. 1 Schematic diagram of electromagnetic stirrer **a** Top view, **b** Front section view

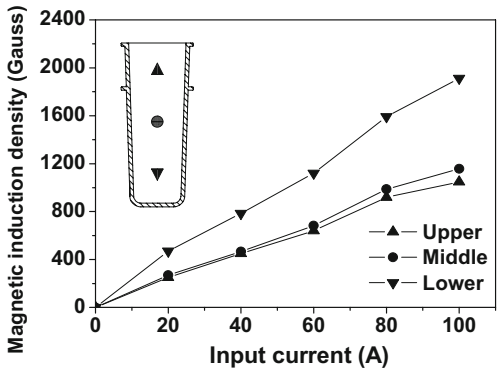

Fig. 2 The measured magnetic flux density at each position in the vessel

Figure 1 is a schematic of the electromagnetic stirrer. The EMS system consists of a melting furnace, an electrical controller, a cooling system in the coil of the stirrer, degassing apparatus of the molten metal, and the vessel to contain the molten metal. The horizontal EMS used in this study was manufactured so that it consisted of three phases and three poles. As each phase was located the circumference of the stirrer such that the current flowed through the coils as shown in Fig. 1, the electromagnetic force was circularly distributed. Damage to the coil from heat radiating from the melt during stirring was prevented by means of a cooling line. The electromagnetic stirring force shears the molten material in semi-solid state and crushes dendrites arising from solidification and thus controls solid particle size. The sleeve was made of a non-magnetic material and so not affected by EMS. The vessel used in EMS was made of a SUS nonmagnetic material and so is also unaffected by EMS, allowing the magnetic field lines to penetrate into the vessel without melting or deforming when contacting molten alloys at temperatures in excess of 700°C.

The electromagnetic force of the stirrer was measured by a Gauss meter throughout each of the parts produced by EMS. Figure 2 shows the measured magnetic induction density and shows the increase of the magnetic induction density as a function of the electric current. The input currents are representative of the strength of the electromagnetic stirring, as can be seen from Fig. 3. A liquid pool was formed on the top surface of the billet stirred at a current of 90 A because the centripetal stirring force increased as the electric current increased.

Therefore, the EMS electric currents used in this study was 60 A, with stirring time varying between 40 and 90 s and a pouring temperature between 15°C and 20°C greater than the liquidus temperature of the alloys. As shown in Fig. 3a and b, the rheological materials fabricated under these experimental conditions encountered no vortices.

3 Indirect rheoforging of A6061 alloy and their results

An indirect semi-solid forging experiment was carried out to investigate the fluidity of the material and the effect on the microstructure of the applied pressure transferred to the material. Figure 4 shows a schematic of an indirect-type rheoforging apparatus. Indirect rheoforging die consisted of upper and lower dies. The rheoforging system was designed so that the lower die was fixed to the lower plate of the press and the punch was connected to the main cylinder to transfer the forging pressure to rheological billet in the die. A cartridge heater was used to maintain the die temperature at 250°C.

Figure 5 shows a schematic of the indirect semi-solid forging process, showing the insertion of the billet into the die, formation, and finally extraction of the product. This test follows the experimental conditions shown in Table 2. Microstructural and mechanical strength test results of materials fabricated by means of EMS using a constant solid fraction but then subjected to varying applied pressures were compared to the test results EMS-fabricated materials using varying solid fractions but all subjected to a constant applied pressure.

To investigate the effect of filling behavior of the materials within the die and the effect of pressing

(a) (b) (c)

Fig. 3 Shapes of the billets during electromagnetic stirring at various current. **a** 25 A, **b** 50 A, **c** 90 A

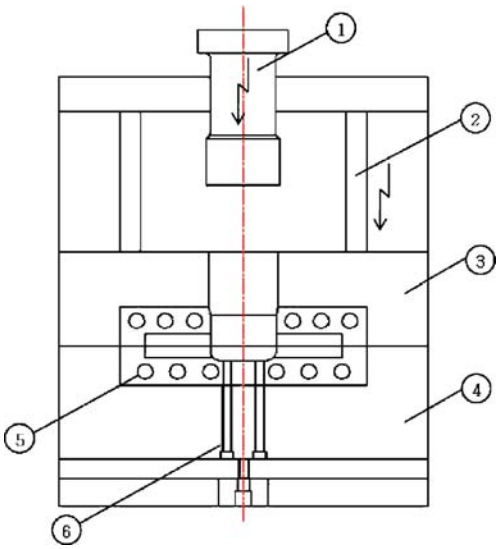

① Punch, ② Cylinder, ③ Upper die,
④ Lower die, ⑤ Heater, ⑥ Ejector pin

Fig. 4 Schematic of indirect-type die set and punch

characteristic upon the resultant mechanical properties of the work piece, the fabricated test specimens were water-quenched. Fabricated specimens were then T6 heat-treated, after which the specimens were tensile tested to evaluate their mechanical properties. Figure 6 depicts positions for the tensile specimens. Position ① represents the area filled by pushing the rheological material and position ② represents the area where the rheological material was in contact with the punch.

Figure 7 shows photographs of the indirect rheoforging samples. The applied pressure was varied from 80 to 220 MPa for experimental conditions 1 through 7 shown in Table 2. The die cavity was filled ever more thoroughly as the applied pressure was increased until the cavity was completely filled under an applied pressure of 150 MPa. Samples 4 through 7 thus all appear virtually identical to the naked eye. Tensile tests were made on the samples rheoforged under experimental condtions 4 through 7. The test results are shown in Fig. 8. The tensile strength at position ① was seen to increase as the applied forging pressure increased, but the tensile strength at position ② is independent of the applied forging pressure. Position ② is subjected to direct pressure from the punch, compressing porosities sufficiently well at 150 MPa so that no additional benefit is seen from larger applied pressures. Position ①, however, depends upon the flow of material into the cavity by means of indirect pressure. Material was seen to fill the die cavity up to position ① when a pressure of 120 MPa was applied at position ②, but the porosities decrecorresponding to microstructure of position (1) where ased and mechanical properties improved only when the applied pressure was increased to 170 MPa or more.

Figure 9 shows the microstructures of indirect-type rheoforged samples fabricated under conditions 2, 4, and 7 as shown in Table 2, all of which have a solid fraction of 50% and used a pouring temperature of 647°C. The samples are subjected to varying applied pressures. Microscopic observation was performed upon the specimens taken at positions (1), (2), (3), and (4). The microstructure of the sample fabricated under condition 7, which exhibited the highest strength, showed uniformly distributed fine and globularized solid particles. The microstructure of the underformed sample (condition 2) exhibited porosities distributed over the entire microstructure due to insufficient transfer of densification pressure to position (1). Unlike the completely formed samples, liquid segregation occurred at position (2), which later moved to the end of the sample as the rheomaterial filled the die cavity under the applied forging pressure. Position (1), in direct contact with the punch, consequently was where most of the liquid was extruded and showed the greatest compression of the solid particles. The tensile test of the specimen taken from position ①, corresponding to microstructure of position (3) where liquid and solid particles were uniformly distributed, resulted in high strength. The tensile test of the specimen taken from position ② corresponding to microstructure of position (1) where microstructure did not vary with increase of applied forging pressure resulted in similar strengths at each experimental condition at above 170 MPa of applied pressure.

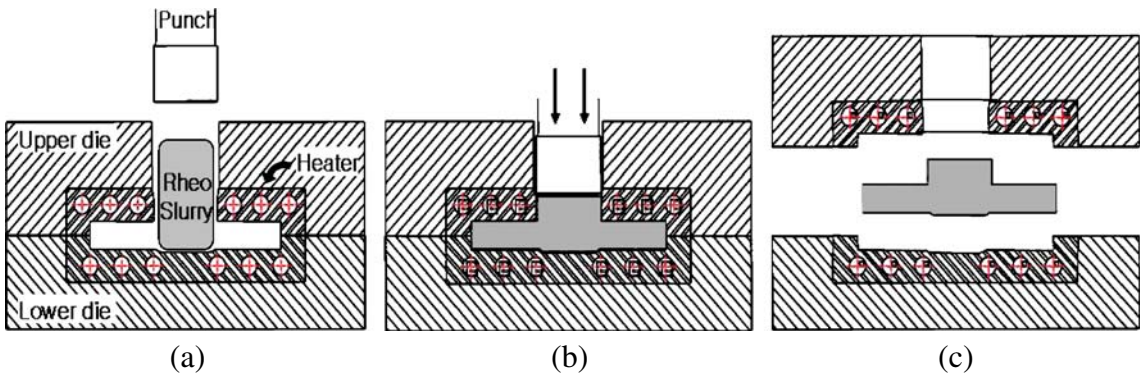

Fig. 5 Schematic of direction indirect-type rheoforging process. Inserting of billet (**a**), forming (**b**), extracting (**c**)

Table 2 Experimental conditions for indirect type rheoforging of Al6061 wrought Al alloy

No.	Pouring temperature (°C)	Stirring current (A)	Forging pressure (MPa)	Holding time (s)
1	647	60	80	20
2	647	60	100	20
3	647	60	120	20
4	647	60	150	20
5	647	60	170	20
6	647	60	200	20
7	647	60	220	20
8	645	60	150	20
9	645	60	170	20
10	645	60	200	20
11	645	60	220	20
12	645	60	250	20
13	640	60	150	20
14	640	60	170	20
15	640	60	200	20
16	640	60	220	20
17	640	60	250	20
18	637	60	220	20
19	640	60	220	20
20	645	60	220	20
21	647	60	220	20
22	651	60	220	20

Figure 10 shows the measured strength of samples fabricated as a function of increasing applied forging pressure, all at a pouring temperature of 645°C and with a solid fraction of 55%. The tensile strength measured at position ① showed a gradual increase with pressure, reaching a maximum value at an applied pressure of 220 MPa. However, the tensile test of the specimen fabricated under experimental condition 12, with an applied pressure of 250 MPa, showed lower strength than the preceding experimental conditions provided. This may be due to the fact that spattering of liquid state material caused by high applied pressure occurred, upsetting the solid fraction. As a result, solid state material stayed in the die cavity, so solid and liquid phase separated and thus mechanical strength decreased. Unlike other experimental conditions, the liquid state of the material at position (4)

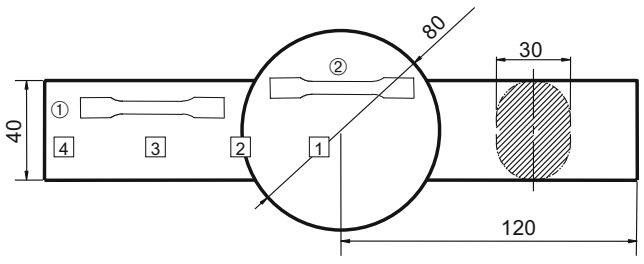

Fig. 6 Positions of specimen to tensile test and observing microstructure

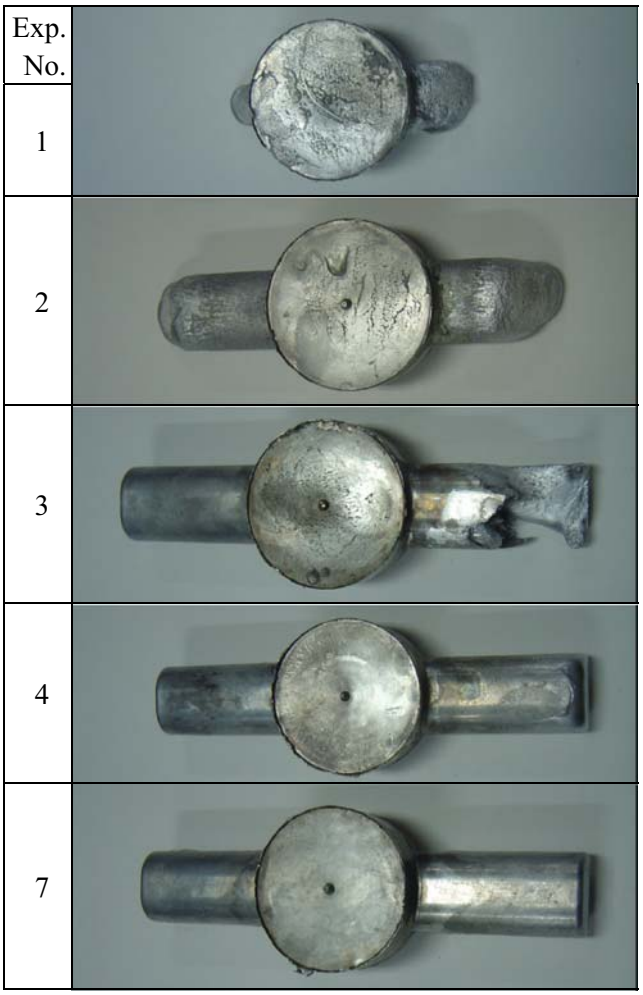

Fig. 7 Photographs of indirection rheoforging samples

was not observed for experimental condition 12. In the case of the two pouring temperatures, 645°C and 647°C, the strength at position ② was uniformly independent of variations in applied pressure. Microstructural observations at position (1) revealed that the grain boundary was indistinct and solid particles occupied the volume, both as a result of the compression.

As shown in Fig. 10, the strength at position ②, corresponding to when the solid phase alone occupied the volume, was lower than the strength at position ① where the solid and liquid phases remained well mixed (Fig. 11).

Figure 12 shows the measured strength of the samples with respect to the applied forging pressure, all at a pouring temperature of 640°C and with a solid fraction of 63%. The strength was seen to increase as the applied pressure was increased. Similar results were obtained under conditions 4 through 7 at a pouring temperature of 647°C and under conditions 8 through 12 at a pouring temperature of 645°C. The strength was seen to decrease as a result of the separation of the solid and liquid phases due to spattering at under conditions 12 and 17. The strength at position ②

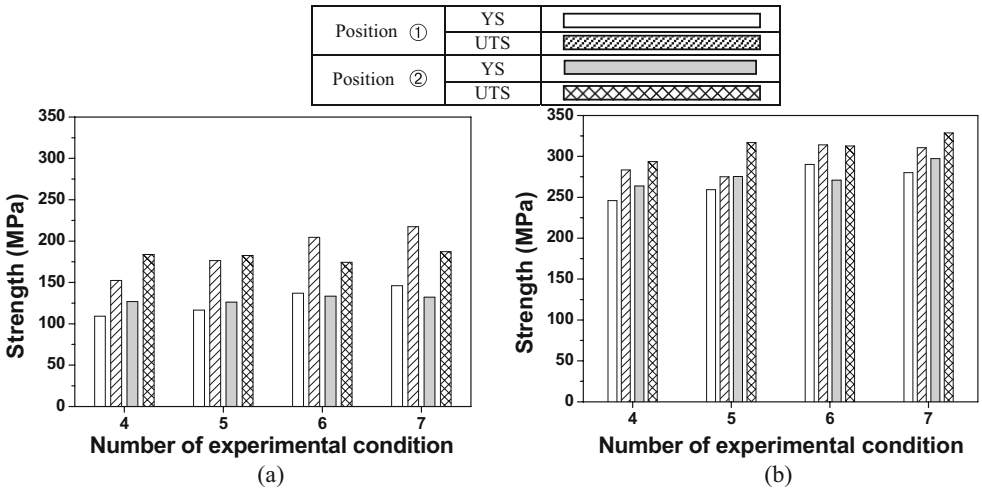

Fig. 8 Tensile strength of 6061 indirect-type rheoforged samples (pouring temperature T_p= 647°C). *YS* yield strength, *UTS* ultimate tensile strength. As fabricated (**a**), after T6 heat treatment (**b**)

showed little variation with applied pressure, this being a result of the fact that the liquid phase had been expressed and only the solid phase remained (Fig. 13).

Figure 14 shows measurements of the tensile strength in which the solid fraction is varied, all under constant applied pressure, as per conditions 18 through 22 shown in Table 2. The strength was not strongly affected by the solid fraction except for condition 18, with a pouring temperature of 637°C. The strength at position ② is similar to the observed strengths seen for other test conditions, whereas the strength at position ① is correspondingly lower. The strength at position ② did not vary with change in solid

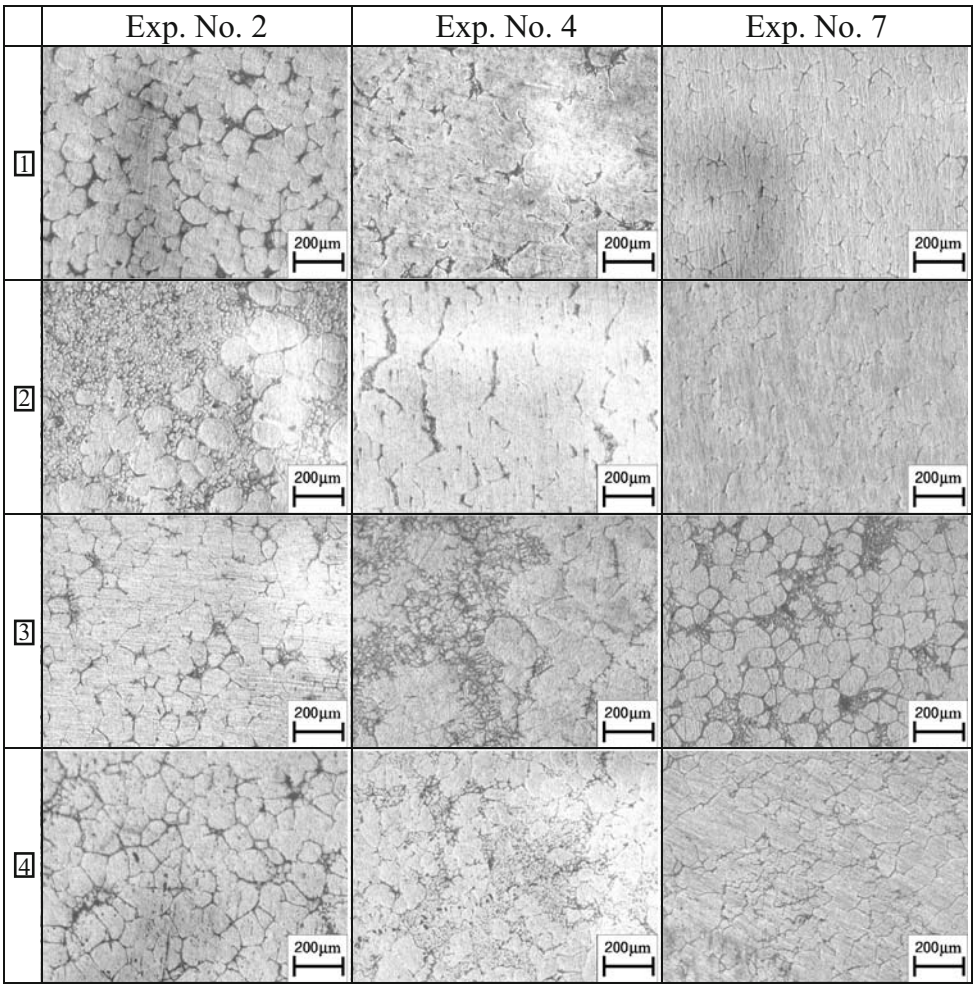

Fig. 9 Microstructure of indirect-type rheoforged sample fabricated by condition 2, 4, and 7 of Table 2 (pouring temperature T_p=647°C)

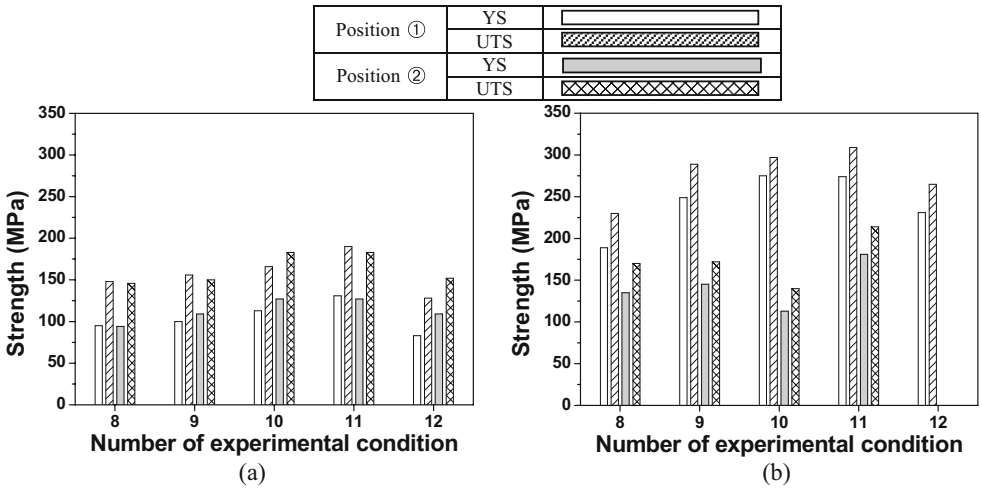

Fig. 10 Tensile strength of 6061 indirect-type rheoforged samples (pouring temperature T_p=645°C). *YS* yield strength, *UTS* ultimate tensile strength. As fabricated (**a**), after T6 heat treatment (**b**)

fraction because the solid particles there were in direct contact with the forge punch and thus directly compressed. Microstructural observation of condition 18 results provided evidence for the change in strength. The microstructure of the sample fabricated under condition 18 large and coarse compared to the microstructure seen for other conditions. Such a coarsened grain may deteriorate the strength. Because the pouring temperature for experimental condition 18 was low at 637°C, it took a longer time to electromagnetically stir the molten alloy during which the material cooled further and the microstructure was coarsened (Fig. 15).

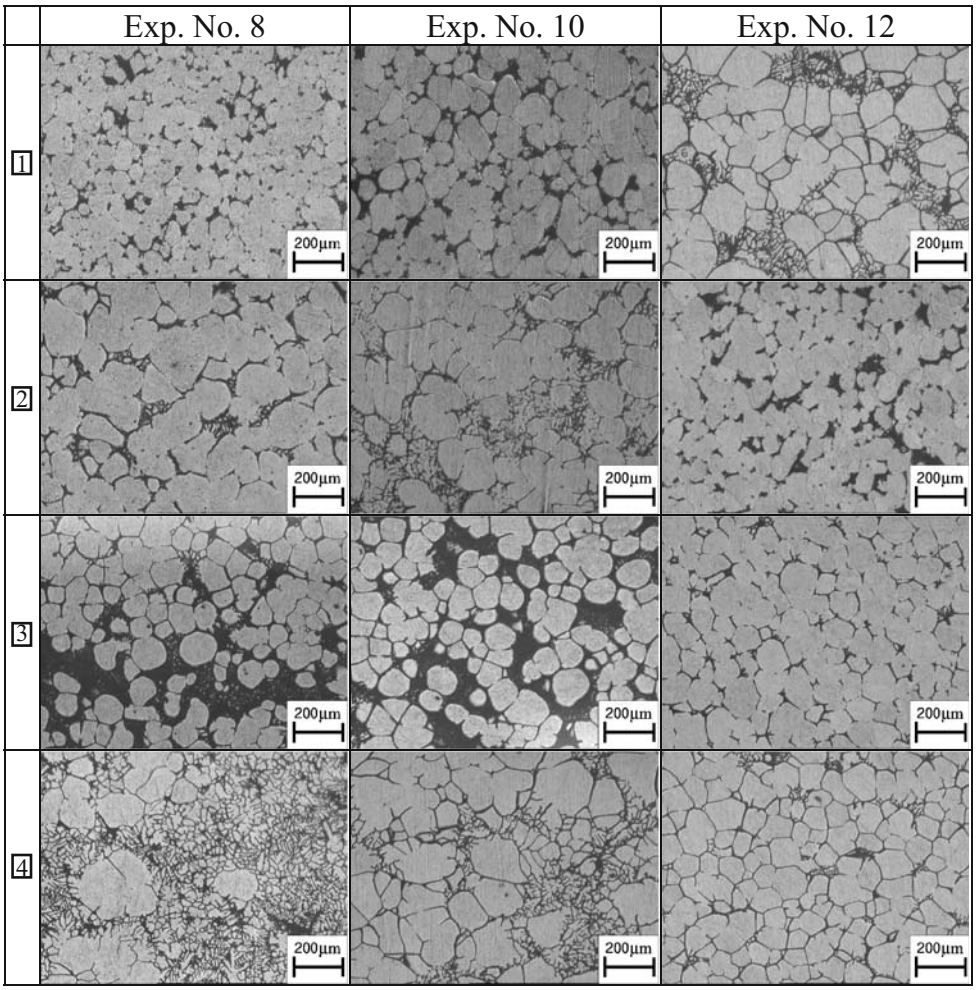

Fig. 11 Microstructure of indirect-type rheoforged sample fabricated by condition 8, 10, and 12 of Table 2 (pouring temperature T_p=645°C)

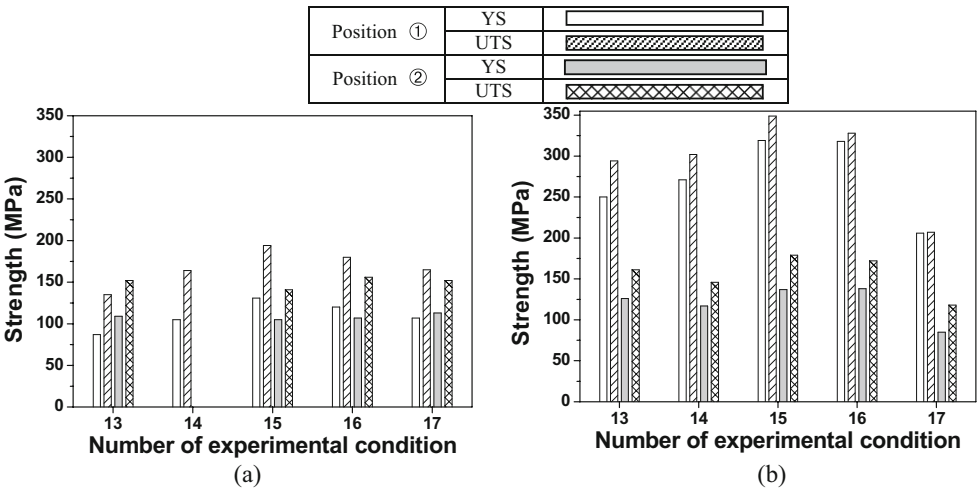

Fig. 12 Tensile strength of 6061 indirect-type rheoforged samples (pouring temperature T_p=640°C). *YS* yield strength, *UTS* ultimate tensile strength. As fabricated (**a**), after T6 heat treatment (**b**)

4 Conclusions

Through indirect rheoforging of wrought aluminum alloys fabricated by EMS, the following conclusions were obtained.

1. By crushing dendrite and rose-type microstructures by EMS at liquid solid coexistent region, fine and globularized microstructure was obtained.
2. Infusion of surface oxides into material and formation of porosities within the material were both prevented, and dendrites were crushed when stirring with a current of 60 A.
3. The rheo-material was pressed into the die cavity, filling it completely, at an applied forging pressure of 150 MPa. To ensure that the densification pressure was

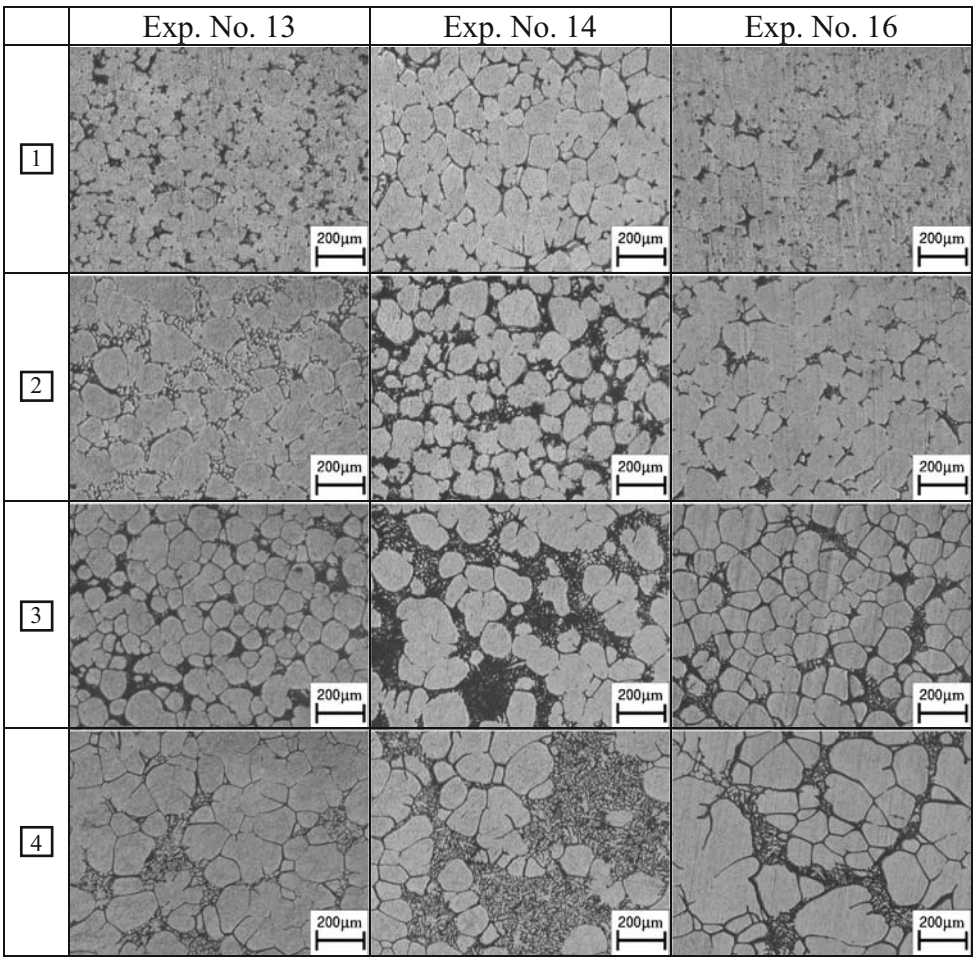

Fig. 13 Microstructure of indirect-type rheoforged sample fabricated by condition 13, 14, and 16 of Table 2 (pouring temperature T_p=640°C)

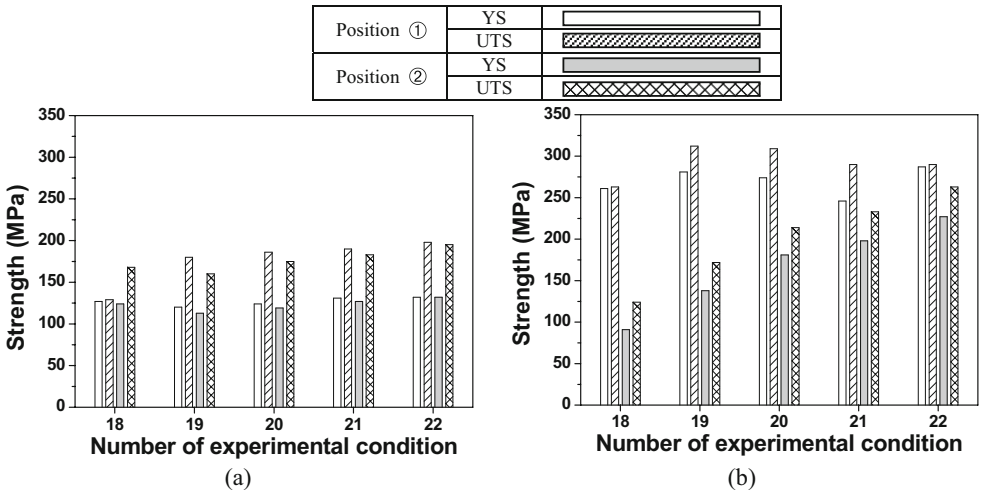

Fig. 14 Tensile strength of 6061 indirect-type rheoforged samples (forging pressure P= 220 MPa). *YS* yield strength, *UTS* ultimate tensile strength. As fabricated (**a**), after T6 heat treatment (**b**)

transferred to the end of the test piece, an applied forging pressure of over 170 MPa was necessary.

4. Liquid segregation, which occurred during indirect rheological forging, degraded the material properties of the product. When liquid segregation occurred significantly during rheoforging of Al6061 alloy, strengths as low as 268 MPa were observed.
5. The material prepared by means of EMS and then rheoforged had a fine and globular microstructure. Rheoforged Al6061 alloy with uniform distribution of

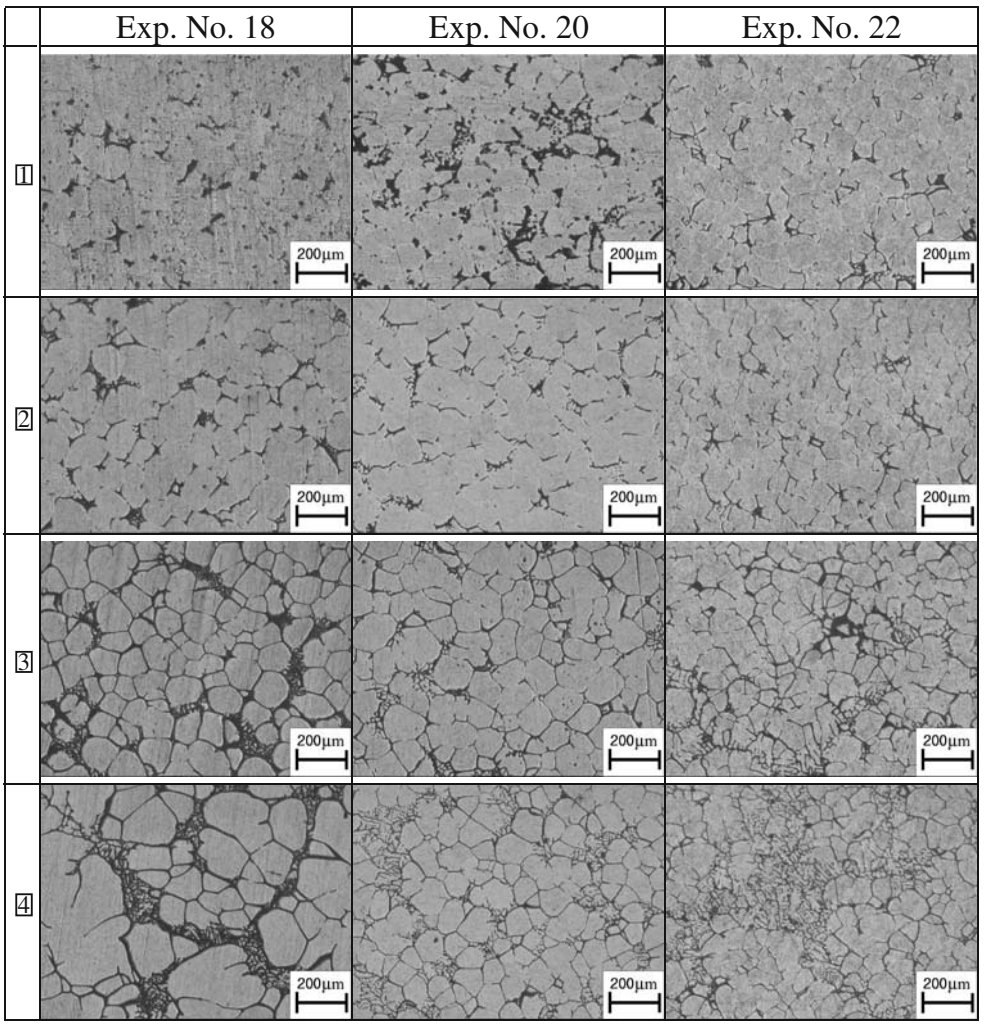

Fig. 15 Microstructure of indirect-type rheoforged sample fabricated by condition 18, 20, and 22 of Table 2 (forging pressure P=220 MPa)

solid and liquid phase (no segregation) within the microstructure showed good mechanical properties with tensile strengths of 341 MPa.

Acknowledgments This work has been supported by the National Core Research Center (NCRC). The authors would like to express our deep gratitude to the Ministry of Science & Technology (MOST) for its financial support.

References

1. Kim S, Lee KH (2004) Product design for high technology of die casting. Journal of the Korean Foundrymen's Society 24(5):251–264
2. Ebisawa M (2004) The latest news of die casting technology. Journal of the Korean Foundrymen's Society 24(2):71–78
3. Kang CG, Choi JC, Bae WB (2000) Semi-solid forming, casting and forging technologies of lightweight materials. Journal of the Korean Society of Precision Engineering 7(4):7–21
4. Spencer DB, Mehrabian R, Flemings MC (1972) Rheological behavior of Sn-15% Pb in the crystallization range. Metall Trans 3:1925–1932
5. Toyoshima S, Takashashi Y (1991) A numerical simulation of forming process for semi-solid materials. ISIJ 3:557–582
6. Hirt G, Cremer R, Winkelmann A, Witulski T, Zillgen M (1994) SSM-forming of usually wrought aluminum alloy. The 3rd International Conference on Semi-Solid Processing of Alloys and Composites, pp 107–116
7. Peng H, Wang SP, Wang N, Cornie JA (1992) Rheomolding-injection molding of semi-solid metals. The 3rd International Conference on Semi-solid Processing of Alloys and Composites, pp 191–200
8. Zoqui EJ, Paes M, Es-Sadiqi E (2002) Macro- and microstructure analysis of SSM A356 produced by electromagnetic stirring. J Mater Process Technol 120:365–373
9. Zoqui EJ, Shehata MT, Paes M, Kao V, Es-Sadiqi E (2002) Morphological evolution of SSM A356 during partial remelting. Mater Sci Eng A 325(Issues 1–2):38–53
10. Zoqui EJ, Gracciolli JI, Lourencato LA (2008) Thixo-formability of AA6063 alloy: conventional production processes versus electromagnetic stirring. J Mater Process Technol 198:155–161
11. Lee SY, Lee JH, Lee YS (2001) Characterization of Al 7075 alloys after cold working and heating in the semi-solid temperature range. J Mater Process Technol 111:42–47
12. Kapranos P, Atkinson HV (2002) Thixoforming 2014, 6082, 7010 and 7075 aluminum wrought alloys. Proceeding of the 7th International Conference on the Semi-Solid Processing of Alloys and Composites, pp 167–171
13. de Freitas ER, Ferracini E Jr, Ferrante M (2004) Microstructure and rheology of an AA2024 aluminium alloy in the semi-solid state, and mechanical properties of a back-extruded part. J Mater Process Technol 146:241–249
14. Liu Z, Mao W, Zhao Z (2006) Research on semi-solid slurry of a hypoeutectic Al–Si alloy prepared by low superheat pouring and weak electromagnetic stirring. Rare Met 25(2):177–183
15. Mao W, Lin H, Bai Y, Gao S (2007) New method for the preparation of semi-solid AlSi7Mg alloy slurry. J Univ Sci Technol Beijing 14(1):56–60
16. Lashkari O, Ghomashchi R, Ajersch F (2007) Deformation behavior of semi-solid A356 Al–Si alloy at low shear rates: the effect of sample size. Mater Sci Eng A 444:198–205
17. Yoon YO, Kim YJ, Kim SK, Jo HH (2005) Microstructure control of AA7075 alloy for thixoextrusion. Journal of the Korean Foundrymen's Society 25(6):249–253
18. Chayong S, Atkinson HV, Kapranos P (2005) Thixoforming 7075 aluminium alloys. Mater Sci Eng A 390(Issues 1–2):3–12
19. Liu D, Atkinson HV, Kapranos P, Jiratticharoean W, Jones H (2003) Microstructural evolution and tensile mechanical properties of thixoformed high performance aluminium alloys. Mater Sci Eng A 361:213–224
20. Liu D, Atkinson HV, Kapranos P, Jones H (2002) Effect of heat treatment on structure and properties of thixoformed wrought alloy 2014. Proceedings of the 7th International Conference on the Semi-Solid Processing of Alloys and Composites, pp 311–316
21. Kim JM, Kim KT, Jung WJ (2002) Semi-solid forming of Al–Zn–Mg–Cu alloy applying low-temperature casting process. Journal of the Korean Foundrymen's Society 22(2):82–88
22. Choi JW, Kwon YD, Lee JW, Lee JH (2001) The effect of cooling rate on the solidification behavior and segregation of 7075 and 7050 aluminum alloys. Journal of the Korean Foundrymen's Society 21(6):343–349